



# Direct and indirect immune effects of CMP-001, a virus-like particle containing a TLR9 agonist

Shakoora A Sabree ,<sup>1,2,3</sup> Andrew P Voigt,<sup>2,4</sup> Sue E Blackwell,<sup>3</sup> Ajaykumar Vishwakarma,<sup>5,6</sup> Michael S Chimenti,<sup>7</sup> Aliasger K Salem,<sup>3,6</sup> George J Weiner <sup>3,6,8</sup>

**To cite:** Sabree SA, Voigt AP, Blackwell SE, *et al.* Direct and indirect immune effects of CMP-001, a virus-like particle containing a TLR9 agonist. *Journal for ImmunoTherapy of Cancer* 2021;**9**:e002484. doi:10.1136/jitc-2021-002484

► Additional supplemental material is published online only. To view, please visit the journal online (<http://dx.doi.org/10.1136/jitc-2021-002484>).

Accepted 04 May 2021

## ABSTRACT

**Background** CMP-001, also known as vidutolimod, is a virus-like particle containing a TLR9 agonist that is showing promise in early clinical trials. Our group previously demonstrated that the immunostimulatory effects of CMP-001 are dependent on an anti-Q $\beta$  antibody response which results in opsonization of CMP-001 and uptake by plasmacytoid dendritic cells (pDCs) that then produce interferon (IFN)- $\alpha$ . IFN- $\alpha$  then leads to an antitumor T-cell response that is responsible for the in vivo efficacy of CMP-001. Here, we explore mechanisms by which the initial effects of CMP-001 on pDCs activate other cells that can contribute to development of an antitumor T-cell response.

**Methods** Uptake of CMP-001 by various peripheral blood mononuclear cell (PBMC) populations and response to anti-Q $\beta$ -coated CMP-001 were evaluated by flow cytometry and single-cell RNA sequencing. Purified monocytes were treated with anti-Q $\beta$ -coated CMP-001 or recombinant IFN- $\alpha$  to evaluate direct and secondary effects of anti-Q $\beta$ -coated CMP-001 on monocytes.

**Results** Monocytes had the highest per cell uptake of anti-Q $\beta$ -coated CMP-001 with lower levels of uptake by pDCs and other cell types. Treatment of PBMCs with anti-Q $\beta$ -coated CMP-001 induced upregulation of IFN-responsive genes including CXCL10, PDL1, and indoleamine-2,3-dioxygenase (IDO) expression by monocytes. Most of the impact of anti-Q $\beta$ -coated CMP-001 on monocytes was indirect and mediated by IFN- $\alpha$ , but uptake of anti-Q $\beta$ -coated CMP-001 altered the monocytic response to IFN- $\alpha$  and resulted in enhanced expression of PDL1, IDO, and CD80 and suppressed expression of CXCL10. These changes included an enhanced ability to induce autologous CD4 T-cell proliferation.

**Conclusions** Anti-Q $\beta$ -coated CMP-001 induces IFN- $\alpha$  production by pDCs which has secondary effects on a variety of cells including monocytes. Uptake of anti-Q $\beta$ -coated CMP-001 by monocytes alters their response to IFN- $\alpha$ , resulting in enhanced expression of PDL1, IDO and CD80 and suppressed expression of CXCL10. Despite aspects of an immunosuppressive phenotype, these monocytes demonstrated increased ability to augment autologous CD4 T-cell proliferation. These findings shed light on the complexity of the mechanism of action of anti-Q $\beta$ -coated CMP-001 and provide insight into pathways that may be targeted to further enhance the efficacy of this novel approach to immunotherapy.

## BACKGROUND

The tumor microenvironment (TME) is extremely complex and is an area of intensive study as we seek to understand the relationship between malignancy and the host immune response. Approaches to modifying the microenvironment with the goal of breaking immune tolerance and enhancing development of a systemic antitumor immune response are ongoing despite our incomplete understanding of how various components of the TME contribute to the success or failure of such therapy. In situ immunization through local manipulation of the TME is showing promise in both preclinical studies and early clinical trials.<sup>1–4</sup>

In situ immunization with TLR9 agonists is particularly attractive as they are potent immunostimulatory agents capable of inducing both innate and adaptive immunity.<sup>5,6</sup> In humans, TLR9 is expressed by plasmacytoid dendritic cells (pDCs) and B cells and can be activated by deoxynucleotides containing unmethylated CpG motifs.<sup>7</sup> Different classes of TLR9 agonists have distinct effects dependent on the cell types they target. Class A TLR9 agonists (CpG-A) impact largely on pDC production of type I interferon (IFN), namely, IFN- $\alpha$  and IFN- $\beta$ .<sup>8,9</sup> Type I IFN then results in downstream changes that can lead to a Th1-skewed cytokine profile and an enhanced antitumor response.<sup>10,11</sup> For example, IFN- $\beta$  can augment cross-presentation of antigen by intratumoral DCs resulting in reactivation of cytolytic CD8 T cells and tumor regression.<sup>11</sup> IFN- $\alpha$  has been shown to modulate antitumor immunity by enhancing generation of monocyte-derived dendritic cells that enhance both innate and adaptive immune activation.<sup>12,13</sup> Class B TLR9 agonists preferentially stimulate B-cell activation.<sup>8,9</sup> This class of TLR9 agonists also display antitumor activity, including activation of effector cells



© Author(s) (or their employer(s)) 2021. Re-use permitted under CC BY-NC. No commercial re-use. See rights and permissions. Published by BMJ.

For numbered affiliations see end of article.

### Correspondence to

Dr George J Weiner;  
george-weiner@uiowa.edu

that facilitate tumor regression.<sup>14,15</sup> Class C TLR9 agonists exhibit features of both classes and can equally activate both pDCs and B cells.<sup>16</sup> Therapeutics based on all three classes are currently in clinical development.<sup>17–19</sup>

One challenge with using CpG-A as a therapeutic agent is its sensitivity to nucleases and short half-life.<sup>20</sup> A novel formulation of a TLR9 agonist encased in a virus-like particle (VLP) derived from the bacteriophage Q $\beta$  coat protein, referred to as CMP-001, was designed in part to overcome this problem and to protect CpG-A from nucleases. This formulation is also different from soluble TLR9 agonists in that the viral protein may provide additional danger signals and alter uptake by antigen-presenting cells, such as pDCs.<sup>21,22</sup> CMP-001, also known as vidutolimod, is currently being tested in a number of clinical trials (clinical trial identifiers: NCT02680184, NCT03084640, NCT03983668) by our group and others with promising preliminary results.<sup>18,23,24</sup>

We recently demonstrated that the efficacy of CMP-001 depends on generation of an anti-Q $\beta$  antibody response which allows for opsonization of CMP-001, uptake by pDCs and subsequent production of IFN- $\alpha$ .<sup>2,3</sup> We also demonstrated the antitumor activity of CMP-001 in a mouse model is T cell dependent.<sup>4</sup> Nevertheless, much remains to be understood about the mechanism of action of CMP-001, how it alters various immune cells found in the TME and how it is the same or different from soluble TLR9 agonists. The current studies were designed to address these questions.

## METHODS

### CMP-001, anti-Q $\beta$ antibody, and other reagents

Unlabeled CMP-001, CMP-001 labeled with Cy5.5, methylated CMP-001 (mCMP-001, CMP-001 produced with methylated oligodeoxynucleotide that lacks TLR9 agonist activity), the G10 oligodeoxynucleotide (unmethylated, lyophilized form), and recombinant anti-Q $\beta$  were provided by Checkmate Pharmaceuticals (Cambridge, Massachusetts, USA). Other sources of anti-Q $\beta$  used in select experiments include humanized anti-Q $\beta$  antibody (cloned from EBV-transformed cells derived from a melanoma patient treated with CMP-001) and heat-inactivated (56°C, 30 min) anti-Q $\beta$ + immune serum (from melanoma patients treated with CMP-001). For IgG+ bead experiments, human polyclonal IgG was purchased from BioXCell (#BE0092) and used to coat Pierce Protein L beads purchased from Thermo Fisher (#88849) as described in the manufacturer's protocol. Recombinant IFN- $\alpha$  was purchased from R&D (#11100–1). Cells were treated with the following concentrations of reagents: 10  $\mu$ g/mL CMP-001, 10  $\mu$ g/mL mCMP-001, 2.5  $\mu$ g/mL G10 (note: CMP-001 is approximately four parts protein and one part DNA), 10  $\mu$ g/mL recombinant anti-Q $\beta$ , 10  $\mu$ g/mL humanized anti-Q $\beta$ , 1.25%

heat-inactivated (56°C, 30 min) anti-Q $\beta$ + immune serum, 10  $\mu$ g/mL IgG+ protein L beads, and/or 1.792 $\times$ 10<sup>4</sup> U/mL recombinant IFN- $\alpha$ .

### Isolation of unfractionated human peripheral blood mononuclear cells (PBMCs)

PBMCs were isolated from leukocyte reduction system cones (DeGowin Blood Center, the University of Iowa) of deidentified healthy donors using Ficoll-Paque gradient centrifugation. Cells were diluted with 20 mL of phosphate-buffered saline (PBS) at room temperature in a 50 mL conical tube. PBMCs were isolated using Ficoll gradient.<sup>25</sup> Buffy coat containing the PBMCs was removed and transferred into a new 50 mL tube. Volume was raised to 50 mL with PBS and tube was spun at 400 $\times$ g for 10 min at room temperature. Supernatant was discarded and 10 mL of ammonium-chloride-potassium buffer (2 L PBS, 16.58 g NH<sub>4</sub>Cl, 2 g KHCO<sub>3</sub>, 74.4 mg Na<sub>2</sub> EDTA, pH 7.2–7.4 with 1 N HCl) was used to lyse red blood cells for 10 min at room temperature. The tube was filled to 50 mL with PBS and spun at 400 $\times$ g for 10 min at room temperature. Human PBMCs were diluted to 1 $\times$ 10<sup>6</sup> cells/mL in Roswell Park Memorial Institute (RPMI) 1640 medium supplemented with 10% heat-inactivated (56°C, 30 min) fetal bovine serum, 1.5 mM L-glutamine, 100 U/mL penicillin, and 100  $\mu$ g/mL streptomycin.

### Isolation of cell fractions

Each indicated cell subset (pDCs, pDC-depleted PBMCs, monocytes, monocyte-depleted PBMCs, and T cells) was isolated via negative selection from fresh unfractionated PBMCs using magnetic coated microbeads. pDCs were isolated using pDC negative isolation kit (Miltenyi Biotec, #130-097-415); pDC-depleted PBMCs were isolated using anti-BDCA-4 Ab-coated magnetic beads (Miltenyi Biotec, #130-090-532); monocytes were isolated using monocyte negative isolation kits (Miltenyi Biotec #130-117-337 for non-flow cytometry experiments and Miltenyi Biotec #130-096-537 for flow cytometry experiments); and monocyte-depleted PBMCs were isolated using anti-CD14 Ab-coated magnetic beads (Miltenyi Biotec, #130-050-201). Briefly, PBMCs were resuspended in magnetic-activated cell sorting buffer (PBS supplemented with 0.5% bovine serum albumin (BSA) and 2 mM EDTA), incubated with Fc receptor block and the appropriate magnetic microbeads as outlined in the accompanied protocols, then washed and passed over a positive selection column in a magnetic field.

### Uptake of fluorescently labeled CMP-001 by various immune cell subsets

Human PBMCs isolated from healthy donors were resuspended at 1 $\times$  10<sup>6</sup> cells/mL then treated with 10  $\mu$ g/mL Cy5.5-labeled CMP-001 plus or minus 10  $\mu$ g/mL anti-Q $\beta$  for 1 hour. For macrophage uptake

experiments, monocytes were isolated from healthy donors, cultured in Nunc UpCell Surface (#174901, Thermo Scientific) six-well culture plates and polarized into classical M1 and M2 macrophages using an established phased-polarization technique.<sup>26</sup> On day 9, macrophages were harvested using temperature reduction, resuspended at  $0.08 \times 10^6$  cells/mL, and treated with  $0.8 \mu\text{g/mL}$  Cy5.5-labeled CMP-001 plus or minus  $0.8 \mu\text{g/mL}$  anti-Q $\beta$  for 1 hour. Uptake of Cy5.5-labeled CMP-001 by various immune cell subsets was evaluated by flow cytometry. Phenotypical characterization of cell subsets included gating on monocytes (CD14<sup>+</sup>), B cells (CD19<sup>+</sup>), T cells (CD3<sup>+</sup>), natural killer (NK) cells (CD3<sup>-</sup>CD56<sup>+</sup>), pDCs (CD14<sup>-</sup>CD19<sup>-</sup>CD3<sup>-</sup>CD56<sup>-</sup>BDCA2<sup>+</sup>), M1 macrophages (CD14<sup>+</sup>CD80<sup>+</sup>CD86<sup>+</sup>), and M2 macrophages (CD14<sup>+</sup>CD163<sup>+</sup>CD206<sup>+</sup>).

### Single-cell RNA sequencing (scRNA-seq) and analysis

#### Sample information and treatment

Human PBMCs were plated in 24-well culture plates (1 mL/well) and treated with CMP-001 ( $10 \mu\text{g/mL}$ ) and humanized anti-Q $\beta$  ( $10 \mu\text{g/mL}$ ) for 24 hours at 37°C. Cells were harvested, spun down for 5 min, and resuspended at a concentration of 1000 cells/ $\mu\text{L}$  in 0.04% non-acetylated BSA (New England Biolabs) in PBS.

#### Barcoding and library construction

Viability analysis was performed using acridine/propidium iodide staining on the Luna software (Logos Biosystems), and all samples were confirmed to be >95% viable (untreated sample=97% viable and treated sample=98.1% viable). Single cells were barcoded with the chromium system using the V.3 single-cell reagent kit (10X Genomics). Barcoded libraries were pooled and sequenced on the HiSeq 4000 platform (Illumina) generating 150-base pair paired-end reads with a requested target recovery of 10,000 cells. cDNA libraries from the samples were qualitatively checked and passed assessment.

#### Computational analysis

FASTQ files were generated from basecall files with the bcl2fastq software (Illumina) provided by the University of Iowa Institute of Human Genetics. Data files were subsequently mapped to the prebuilt GRCh38 genome with Cell Ranger V.3.0.1.<sup>27</sup> After initial mapping, canonical correlation analysis was performed to integrate the dataset,<sup>28</sup> and clustering was performed based on integrated sets using the Seurat R Package V.3.0.2.<sup>29</sup> Cells with unique gene counts fewer than 300 or more than 4000 per cell were eliminated (to eliminate low-quality cells and doublets), as were cells that had more than 25% of expressed genes identified as mitochondria genes. A total of 17,280 cells were recovered after filtering and were visualized with the dimensionality reduction

technique uniform manifold approximation and projection. Differential expression analyses were performed with the following criteria: logFC difference of 0.1 and percent of cells expressing a difference of 25%. Cell-type prioritization analysis was performed using 'Augur' V.1.0.2, R V.4.0.3 (<https://github.com/neurorestore/Augur/>) with the 'calculate\_auc' function in pairwise analysis mode.

### Neutralization experiments

PBMCs were isolated, diluted to  $1 \times 10^6$  cells/mL and treated with  $10 \mu\text{g/mL}$  anti-Q $\beta$ -coated CMP-001 with or without antihuman IFN- $\alpha$  ( $5 \mu\text{g/mL}$ , MMHA-2, Cat #211002; Thermo Fisher), antihuman IFNAR2 ( $5 \mu\text{g/mL}$ , MMHAR-2; PBL; Cat #21385-1), mouse IgG2a, kappa isotype control ( $5 \mu\text{g/mL}$ , Cat# 16-4724-85; Thermo Fisher), or mouse IgG1, kappa isotype control ( $5 \mu\text{g/mL}$ , Cat #14471482; Thermo Fisher) for 24 hours. For CD32a neutralization experiments, monocytes were diluted to  $1 \times 10^6$  cells/mL and treated with  $50 \mu\text{g/mL}$  anti-CD32a (R&D, #AF1875) or isotype control (R&D, #AB-108-C) for 15 min followed by treatment with  $10 \mu\text{g/mL}$  anti-Q $\beta$ -coated CMP-001 and  $1.792 \times 10^4$  U/mL recombinant IFN- $\alpha$  for 18–20 hours.

### Coculture and transwell assays

Human pDCs and monocytes were isolated as previously described. To enhance the purity of pDCs, pDCs were passed over a second positive selection column. To enhance the purity of monocytes, any lingering pDCs were removed from the monocyte fraction by passing them over a pDC selection column. Flow cytometry was used to confirm purity of cell fractions. For coculture experiments, pDCs were cultured directly with monocytes. Cells were treated with respective drugs and after a 24-hour incubation period, the supernatant was harvested and analyzed for CXCL10 production by ELISA. For transwell experiments, pDCs and monocytes were separated by a  $0.4 \mu\text{m}$  pore polycarbonate membrane insert available through Corning (Cat: #3413). Membranes were presoaked with  $100 \mu\text{L}$  of RPMI for 1 hour prior to plating cells. pDCs were treated with respective drugs, and after a 24-hour incubation period, the supernatant was harvested from monocytes in the bottom well and analyzed for CXCL10 production by ELISA.

### IFN- $\alpha$ and CXCL10 ELISAs

Human IFN- $\alpha$  and CXCL10 ELISAs were purchased from PBL Assay Science (#41100-2), R&D Systems (#SIP100), and Thermo Fisher (#KAC2361). Plates were read at 450 nm (with wavelength correction by subtracting readings at 540 nm) with a Molecular Devices Kinetic microplate reader and analyzed with SOFTmax computer software (Molecular Devices, Sunnyvale, California, USA).

## Flow cytometry

Unfractionated PBMCs and monocytes were isolated and treated as indicated. After incubation, cells were harvested and washed with PBS prior to staining with Zombie Aqua Viability Dye (Biolegend #423102). Cells were then stained with commercial antibodies against CD14 (Biolegend #301822, #325618, and #301830), PDL1 (Biolegend #329740), BDCA2 (Miltenyi Biotec #130-113-654), BDCA4 (Miltenyi Biotec #130-118-893), CD3 (Thermo Fisher #17-0036-42), CD4 (Biolegend #317426), CD8 (BD Biosciences #555367), CD56 (Biolegend #557699), CD19 (Biolegend #5577835), CD80 (Biolegend #305218), CD86 (Biolegend #374206), CD163 (Biolegend #333617), and CD206 (Biolegend #321120) at 4°C for 15 min. Antihuman CD16/32 was included to block Fc receptors. For intracellular staining, cells were fixed and permeabilized with eBioscience Intracellular Fixation and Permeabilization Buffer set (Thermo Fisher Scientific #88-8824-00), followed by staining with antibodies against indoleamine-2,3-dioxygenase (IDO; Thermo Fisher Scientific #50-112-9044) and CXCL10 (Miltenyi Biotec #130-104-963). Median fluorescence intensity for all markers were reported. All samples were assessed within 48 hours on the Becton Dickson LSR II flow cytometer. Data were analyzed using FlowJo V.10.2.

## T-cell proliferation

Monocytes and T cells were isolated and any remaining pDCs were removed by passing them over a pDC selection column. Monocytes were treated as indicated for 18–20 hours. The next day, 10 million autologous T

cells were labeled with carboxyfluorescein succinimidyl ester (CFSE; #C34554, 1:1000 dilution; Thermo Fisher) in PBS for 3 min at room temperature in the dark, followed by 7 min at 37°C in the dark. Cells were washed twice with PBS. Autologous CFSE-labeled T cells were added to monocyte cultures at a ratio of 10:1 (T cell:monocyte). After 4 days, CFSE dilution as a measure of T-cell proliferation was determined by flow cytometry.

## Statistical analysis

Data were analyzed using GraphPad Prism V.8.2.1. Parametric tests including Student's paired t-test, mixed-effects analysis, and two-way and one-way analyses of variance with multiple comparisons test were used to assess statistical significance. A p value of <0.05 was used for all experiments.

## RESULTS

### Uptake of CMP-001 is most pronounced in monocytes

Initial studies evaluated uptake of fluorescently labeled CMP-001 plus or minus anti-Q $\beta$  by various PBMC cell populations. As illustrated in [figure 1](#), monocytes had the greatest uptake of CMP-001 labeled with Cy5.5 on a per cell basis when anti-Q $\beta$  was present, with detectable but considerably lower uptake of CMP-001 by other cell types, including pDCs, B cells and NK cells ([figure 1A](#)). Thus, although pDCs are central in orchestrating the immune response to CMP-001, monocytes are more effective at phagocytosis of such particles. Monocytes were polarized into classical M1 and M2 macrophages, with the understanding that

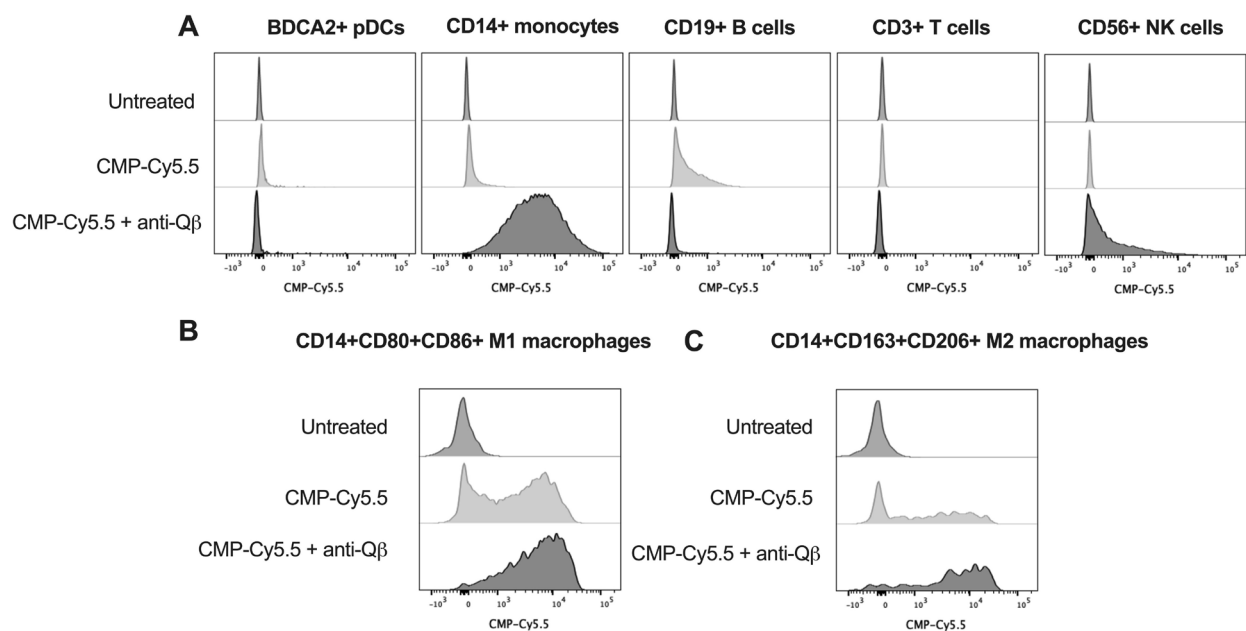


**Figure 1** Uptake of fluorescently labeled CMP-001 by various immune cell subsets. Unfractionated human peripheral blood mononuclear cells (A) or monocytes polarized into classical M1 (B) and M2 (C) macrophages were treated with Cy5.5-labeled CMP-001 plus or minus anti-Q $\beta$  for 1 hour. Cells were stained for unique surface markers and analyzed via flow cytometry. Data are representative of two to three individual experiments. NK, natural killer.

such polarization is an oversimplification of the broad variety of myeloid cell populations present within the TME. Both were able to phagocytose opsonized CMP-001, with greater per cell uptake by M1 macrophages (figure 1B,C).

### scRNA-seq demonstrates anti-Q $\beta$ -coated CMP-001 induces increased expression of IFN response genes, particularly in monocytes

The finding that pDCs are central to the immune response induced by CMP-001, but that monocytes take up more particles on a per cell basis, suggests CMP-001 can have both direct and indirect effects on various immune cell populations. To better understand these effects, PBMCs from normal donors (n=2) were treated with anti-Q $\beta$ -coated CMP-001 for 24 hours and analyzed by scRNA-seq. After initial mapping and normalization, clustering was performed based on integrated datasets (figure 2A) and segregated to compare gene expression by treated and untreated cells (figure 2B,C). Classic cell-type surface markers based on published data<sup>30 31</sup> were used to identify clusters of immune cells (figure 2D and online supplemental figure 1). Ingenuity pathway analysis was used to assess genes differentially expressed by treated and untreated cells and demonstrated a strong type I IFN response signature in response to anti-Q $\beta$ -coated CMP-001 in various cell types (online supplemental figure 2 and online supplemental figure 3). Distinct gene expression patterns were found for each cell type following anti-Q $\beta$ -coated CMP-001 treatment, with particularly notable changes in monocytes (online supplemental figure 2). Augur analysis, a cell-type prioritization tool that uses machine learning to identify which cell clusters are most affected by a particular treatment independent of cluster size and differential expression,<sup>32</sup> identified monocytes as being the most responsive to anti-Q $\beta$ -coated CMP-001 treatment of PBMCs (online supplemental figure 4). To further explore the effect of anti-Q $\beta$ -coated CMP-001 on the gene expression profile of monocytes, differentially expressed genes were analyzed, comparing treated and untreated monocytes (cluster 5) (figure 2E). The most profound changes were associated with type I and type II IFN responses (figure 2F). An ingenuity pathway analysis also identified changes in genes involved in communication between innate and adaptive immune cells and antigen presentation (figure 2G). These included a number of genes that can impact on development of an antitumor T-cell response, including but not limited to interleukin-27, CCL7, CCL8, CD80, CD274 (PDL1), IDO1 (IDO), CXCL11 and CXCL10.<sup>3 33–39</sup> Expression of these genes across the various cell types showed treatment-related expression changes primarily, but not exclusively, in monocytes (figure 2H–K and online supplemental figure 5). These data are accessible for viewing via an interactive web interface (<https://cmp001.shinyapps.io/cmp001/>) using the cellcurator R package.<sup>40</sup>

### CMP-001-mediated induction of CXCL10 in monocytes is dependent on pDC-derived type I IFN

As previously reported<sup>10 39 41 42</sup> and illustrated in the scRNA-seq studies at the level of gene expression, TLR9 agonists can induce CXCL10, IDO and PDL1 expression by monocytes in a type I IFN-dependent manner.<sup>39 41 42</sup> To further explore the direct versus indirect effects of CMP-001 on CXCL10 production by monocytes, unfractionated PBMCs, monocyte-depleted PBMCs, and isolated monocytes were treated with anti-Q $\beta$ -coated CMP-001 for 24 hours, and the supernatant was evaluated for CXCL10. As illustrated in figure 3, anti-Q $\beta$ -coated CMP-001 induced production of CXCL10 by unfractionated PBMCs (figure 3A). Production of CXCL10 was abrogated but not completely abolished by monocyte depletion (figure 3A), consistent with the ability of TLR9-mediated signaling cascades to stimulate CXCL10 production by monocytes and to a lesser extent by other cell populations, such as B cells.<sup>43</sup> Monocytes and pDCs alone each failed to produce CXCL10 in response to anti-Q $\beta$ -coated CMP-001 (figure 3B), but the combination of monocytes and pDCs produced robust CXCL10 levels (figure 3B). Cell-to-cell contact was not required for pDCs to induce CXCL10 production by monocytes as determined by studies using a transwell system (figure 3C). For these studies, pDCs were treated and plated above monocytes for 24 hours. The supernatant from monocytes in the bottom well was evaluated for CXCL10. To determine which pDC-derived soluble factors might be contributing to CXCL10 production by monocytes, the supernatant from pDCs treated with anti-Q $\beta$ -coated CMP-001 was analyzed for IFN- $\alpha$  and IFN- $\beta$ , known inducers of CXCL10.<sup>35 44–47</sup> Both IFN- $\alpha$  and IFN- $\beta$  were significantly increased in supernatant from pDCs treated with anti-Q $\beta$ -coated CMP-001 (figure 3D,E). Neutralization of IFN- $\alpha$  alone had minimal impact on CXCL10 levels (figure 3F), whereas blocking IFNAR2, the high-affinity subunit of IFNAR that recognizes multiple types of type I IFN,<sup>48</sup> significantly abrogated the ability of anti-Q $\beta$ -coated CMP-001 to induce CXCL10 production by PBMCs (figure 3G).

### Production of type I IFN in response to anti-Q $\beta$ -coated CMP-001 enhances expression of IDO and PDL1 by monocytes

The downstream effects of CMP-001-induced type I IFN production were explored further by assessing protein expression of IDO (cytoplasmic) and PDL1 (surface) by monocytes in response to treatment of unfractionated PBMCs with recombinant IFN- $\alpha$ . As illustrated in figure 4, anti-Q $\beta$ -coated CMP-001 enhanced expression of IDO and PDL1 by monocytes (figure 4A,D). Antibodies against IFNAR2 blocked anti-Q $\beta$ -coated CMP-001-mediated expression of IDO (figure 4B). A similar yet non-significant trend was seen with PDL1 expression (figure 4E), suggesting that factors other than type I IFN contribute to enhanced expression of this molecule. Treatment of unfractionated PBMCs with recombinant IFN- $\alpha$  recapitulated the effect of anti-Q $\beta$ -coated CMP-001

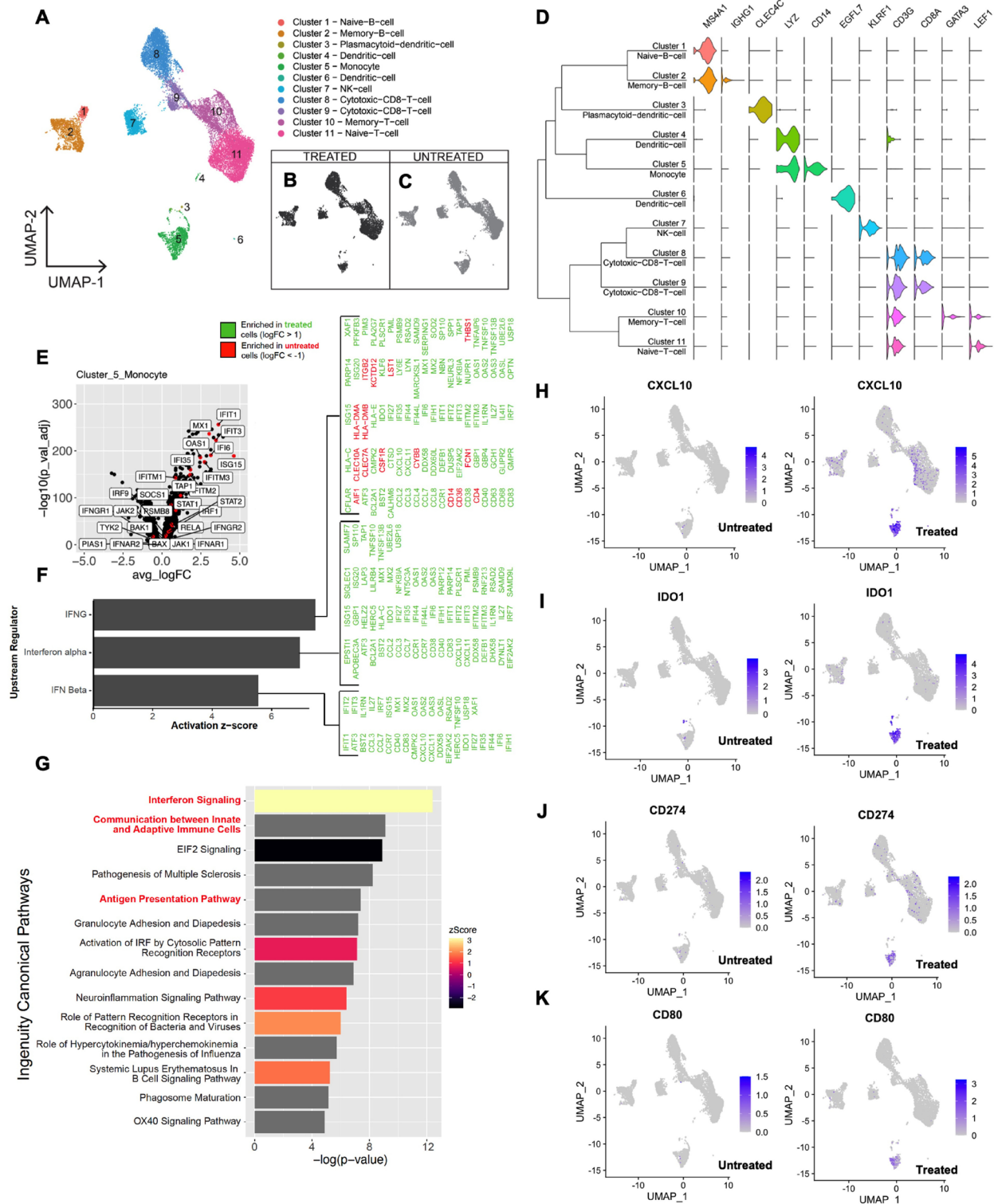


**Figure 2** scRNA-seq of PBMCs treated with anti-Q $\beta$ -coated CMP-001 demonstrates upregulation of genes in monocytes that can impact on T-cell function, including those in the IFN pathway. scRNA-seq was performed on unfractionated normal donor PBMCs treated with and without anti-Q $\beta$ -coated CMP-001. Data from one of two similar experiments are shown. (A) Clustering of merged datasets. (B) Clustering of treated cells. (C) Clustering of untreated cells. (D) Violin plots of classic cell-type surface markers. (E) Volcano plot of differentially expressed genes in monocytes (cluster 5) following anti-Q $\beta$ -coated CMP-001 treatment. For most genes, treatment resulted in positive logFCs. (F) Ingenuity pathway analysis of potential upstream regulators of differentially expressed genes in monocytes following anti-Q $\beta$ -coated CMP-001 treatment. (G) Ingenuity pathway analysis of upregulated signaling pathways in monocytes following anti-Q $\beta$ -coated CMP-001 treatment. UMAP plots of CXCL10 (H), IDO1 (IDO) (I), CD274 (PDL1) (J), and CD80 (K) untreated (left) and treated with anti-Q $\beta$ -coated CMP-001 (right). IRF, interferon regulatory factor; IFN, interferon; PBMC, peripheral blood mononuclear cell; scRNA-seq, single-cell RNA sequencing; UMAP, uniform manifold approximation and projection; IDO, indoleamine-2,3-dioxygenase.

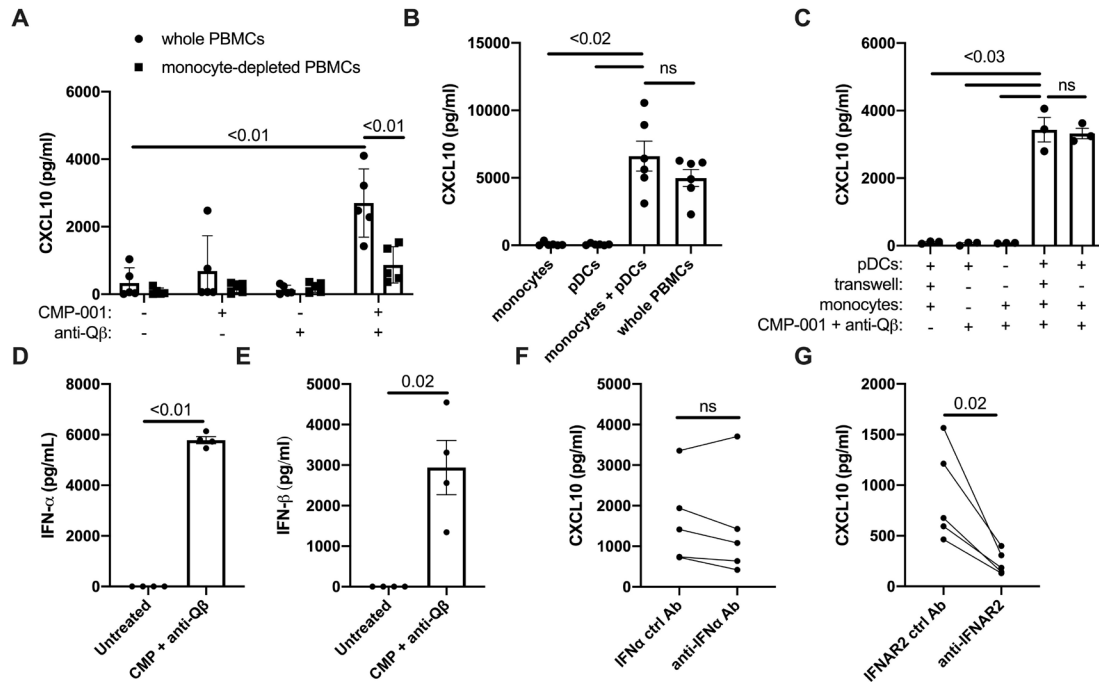


**Figure 3** Anti-Q $\beta$ -coated CMP-001-mediated induction of CXCL10 is dependent on monocytes and pDC-derived type I IFN. Various cell populations were treated with CMP-001 with and without anti-Q $\beta$  for 24 hours and supernatant evaluated for CXCL10, IFN- $\alpha$ , and IFN- $\beta$ . (A) CXCL10 production in response to anti-Q $\beta$ -coated CMP-001 by PBMCs with and without monocyte depletion. (B) CXCL10 production by monocytes combined with pDCs in response to anti-Q $\beta$ -coated CMP-001. (C) CXCL10 production in response to anti-Q $\beta$ -coated CMP-001 by monocytes plus pDCs when cells were placed on the same (-) or opposite (+) sides of a transwell. (D) Production of IFN- $\alpha$  by pDCs treated with anti-Q $\beta$ -coated CMP-001. (E) Production of IFN- $\beta$  by pDCs treated with anti-Q $\beta$ -coated CMP-001. (F) Impact of antibody blocking of IFN- $\alpha$  on CXCL10 production by PBMCs treated with anti-Q $\beta$ -coated CMP-001. (G) Impact of antibody blocking of IFNAR2 on CXCL10 production by PBMCs treated with anti-Q $\beta$ -coated CMP-001. Graphs depict means $\pm$ SEM. Statistical significance was determined using two-way ANOVA with multiple comparisons test (A), one-way ANOVA with multiple comparisons test (B,C), and paired t-test (D-G) with  $\alpha=0.05$  ( $n=3-6$ ). ANOVA, analysis of variance; IFN, interferon; ns, not significant; PBMC, peripheral blood mononuclear cell; pDC, plasmacytoid dendritic cell.

treatment and induced IDO and PDL1 expression by monocytes (figure 4C,F).

#### Phagocytosis of anti-Q $\beta$ -coated CMP-001 by monocytes enhances expression of PDL1 and IDO and suppresses expression of CXCL10 in response to IFN- $\alpha$

To confirm pDC-derived type I IFN acts directly on monocytes, purified monocytes were treated with recombinant IFN- $\alpha$ . As expected, direct stimulation of monocytes with IFN- $\alpha$  enhanced IDO, PDL1, and CXCL10 expression (figure 5A,E,I). To assess whether phagocytosis of CMP-001 by monocytes impacts their response to IFN- $\alpha$ , monocytes were treated with CMP-001 plus or minus anti-Q $\beta$  in the presence or absence of IFN- $\alpha$  for 18–20 hours. Phagocytosis of anti-Q $\beta$ -coated CMP-001 in the absence of IFN- $\alpha$  stimulation had a modest yet statistically significant impact on monocyte expression of IDO, PDL1, and CXCL10 (online supplemental figure 6). Particle phagocytosis also induced changes in monocyte light scatter and size, which may have contributed to the observed modest phenotypical changes. Such changes were not seen in response to treatment with soluble TLR9 agonist, G10 (online supplemental figure 6).

While the direct effect of anti-Q $\beta$ -coated CMP-001 on monocytes was modest, such treatment did have a profound impact on how monocytes responded to IFN- $\alpha$ . Monocytes that had phagocytosed anti-Q $\beta$ -coated CMP-001 responded to IFN- $\alpha$  with enhanced expression of IDO and PDL1 and reduced expression of CXCL10 (figure 5B,F,J). These changes did not occur after treatment of monocytes with unopsonized CMP-001 in the presence of IFN- $\alpha$  (online supplemental figure 7). Phagocytosis of anti-Q $\beta$ -coated CMP-001 had a similar although not statistically significant trend on soluble levels of CXCL10 within the supernatant (online supplemental figure 8).

To assess which component of CMP-001 was responsible for altering the response of monocytes to IFN- $\alpha$ , monocytes were treated with IFN- $\alpha$  along with a VLP composed of a Q $\beta$  capsid encasing a methylated oligodeoxynucleotide that does not function as a TLR9 agonist (mCMP-001), with G10 that is a soluble TLR9 agonist, or with IgG+ protein L beads. Monocytes treated with anti-Q $\beta$ -coated mCMP-001 (figure 5C,G,K) or IgG+ protein L beads (figure 5D,H,L) responded to IFN- $\alpha$  in a manner

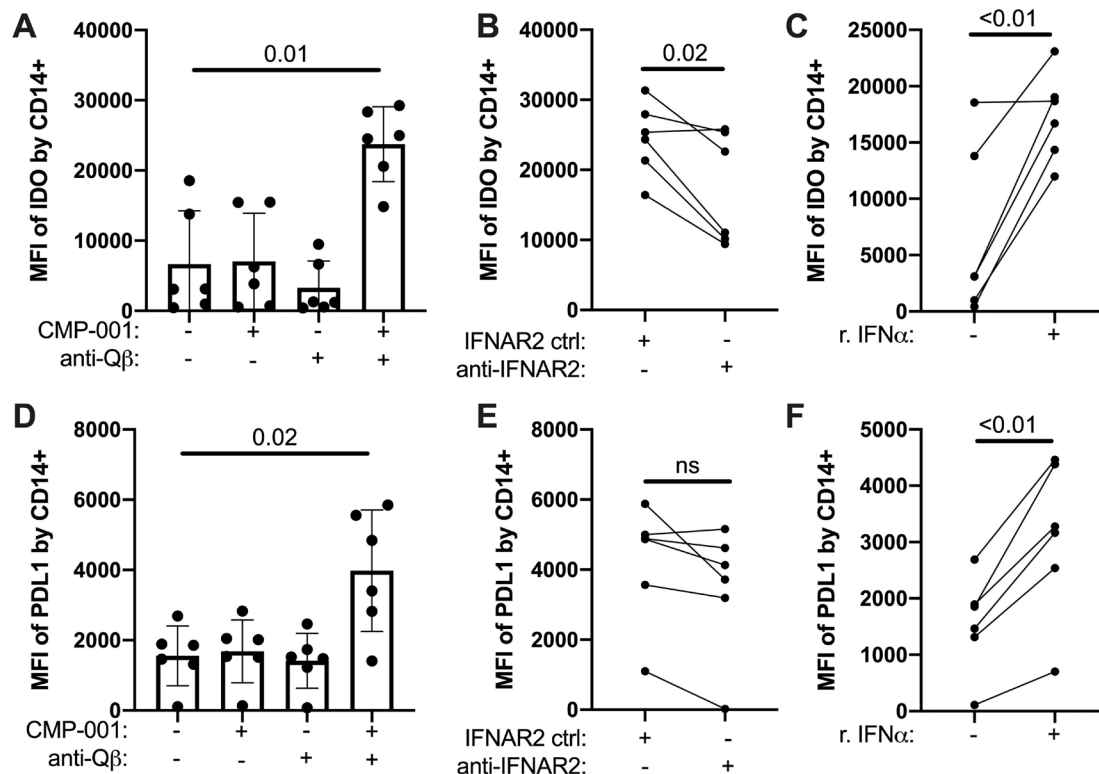


**Figure 4** Anti-Q $\beta$ -coated CMP-001 enhanced expression of IDO and PDL1 by monocytes is dependent on type I IFN. Unfractionated PBMCs from healthy donors were treated with CMP-001 with and without anti-Q $\beta$ , and expression of cytoplasmic IDO and surface PDL1 by monocytes was determined by flow cytometry. (A,D) Expression of IDO and PDL1 induced by CMP-001 with and without anti-Q $\beta$ . (B,E) Impact of antibody blocking of IFNAR2 on expression of IDO and PDL1 induced by anti-Q $\beta$ -coated CMP-001. (C,F) Expression of IDO and PDL1 induced by recombinant IFN- $\alpha$ . Graphs illustrate expression (MFI) of IDO and PDL1 on Zombie Aqua negative CD14 $^+$  cells. Statistical significance was determined using one-way analysis of variance with multiple comparisons test (A,D) and paired t-test (B,C,E,F) with  $\alpha=0.05$  ( $n=6$ ). IFN, interferon; MFI, median fluorescence intensity; ns, not significant; PBMC, peripheral blood mononuclear cell; IDO, indoleamine-2,3-dioxygenase.

similar to that seen with anti-Q $\beta$ -coated CMP-001, while G10 had no identifiable effect on monocyte phenotype (figure 5C,G,K). This suggests Fc receptor-mediated phagocytosis of particles by monocytes, and not the TLR9 agonist itself, modifies the monocytic response to IFN- $\alpha$  including increased IDO and PDL1 expression and suppressed CXCL10 expression.

Blockade of CD32a, the Fc receptor that facilitates uptake of immune complexes,<sup>49</sup> inhibited phagocytosis of anti-Q $\beta$ -coated CMP-001 by monocytes (figure 6A) and blocked the ability of anti-Q $\beta$ -coated CMP-001 to modulate expression of PDL1 and CXCL10 by monocytes in response to IFN- $\alpha$  (figure 6B,C). Unexpectedly, CD32a blockade enhanced expression of IDO (figure 6D). Further experiments were done to assess the role of CD64 in the monocytic response to IFN- $\alpha$  and anti-Q $\beta$ -coated CMP-001. As illustrated in figure 6E, CD64 cross-linking via anti-CD64 enhanced expression of IDO in response to IFN- $\alpha$  even in the absence of particles. This interplay of IFN- $\alpha$ , multiple Fc receptors, and anti-Q $\beta$ -coated CMP-001 likely explains the complex phenotypical changes seen in monocytes in response to anti-Q $\beta$ -coated CMP-001.

#### Monocytes treated with anti-Q $\beta$ -coated CMP-001 and IFN- $\alpha$ upregulate CD80 expression and induce autologous CD4 T-cell proliferation

Additional studies were done to assess the functional impact of the complex changes to monocytes induced by anti-Q $\beta$ -coated CMP-001. Surface expression of CD80 increased after monocytes phagocytosed anti-Q $\beta$ -coated CMP-001 in the context of IFN- $\alpha$  (figure 7A). Such monocytes enhanced autologous CD3 $^+$  T-cell proliferation (figure 7B). These findings were not due to a direct impact of anti-Q $\beta$ -coated CMP-001 and/or IFN- $\alpha$  on T-cell proliferation as they were dependent on the presence of monocytes (figure 7C). Most of the proliferation occurred in CD4 $^+$  T cells (figure 7E), which is consistent with our prior demonstration that CMP-001 induces proliferation of CD4 $^+$  T cells in the draining lymph nodes of mice *in vivo*.<sup>3</sup>

#### DISCUSSION

CMP-001, also known as vidutolimod, is a VLP containing a class A TLR9 agonist. Intratumoral injection of CMP-001, with the goal of altering the TME and successfully inducing



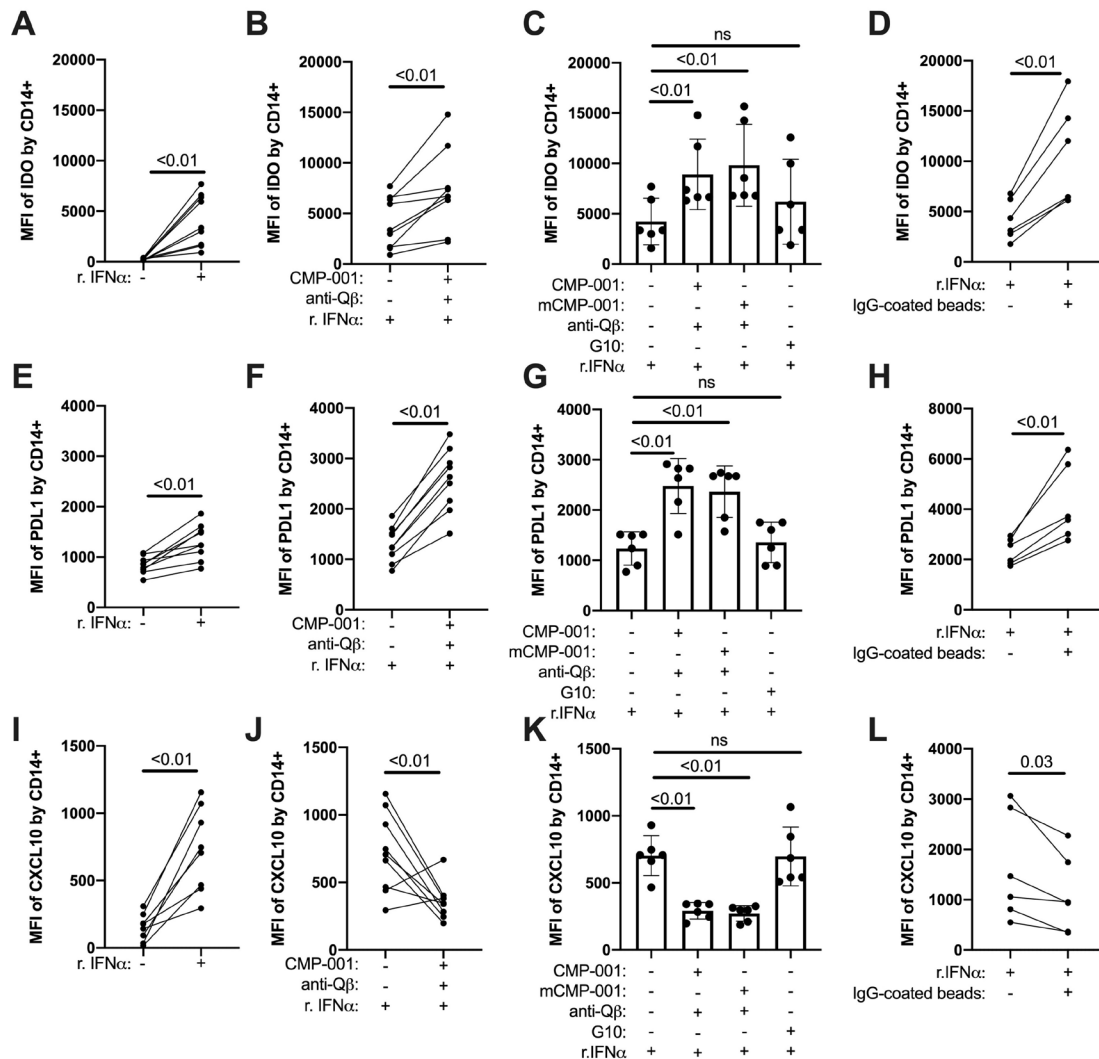


**Figure 5** Phagocytosis by monocytes of antibody-coated particles alters their response to IFN- $\alpha$ . Monocytes from healthy donors were treated with recombinant IFN- $\alpha$  plus or minus anti-Q $\beta$ -coated CMP-001, anti-Q $\beta$ -coated methylated CMP-001 (mCMP-001), G10 (soluble TLR9 agonist) or IgG +proteinL beads for 18–20 hours. Expression of cytoplasmic IDO and CXCL10 and surface PDL1 was determined by flow cytometry. (A,E,I) Impact of recombinant IFN- $\alpha$  on IDO, PDL1, and CXCL10 expression by monocytes. (B,F,J) Impact of anti-Q $\beta$ -coated CMP-001 on IDO, PDL1, and CXCL10 expression by monocytes in response to IFN- $\alpha$ . (C,G,K) Impact of anti-Q $\beta$ -coated CMP-001, anti-Q $\beta$ -coated mCMP-001, or G10 on IDO, PDL1, and CXCL10 expression by monocytes in response to IFN- $\alpha$ . (D,H,L) Impact of IgG+ protein L beads on IDO, PDL1, and CXCL10 expression by monocytes in response to IFN- $\alpha$ . Statistical significance was determined using one-way analysis of variance with multiple comparisons test and paired t-test with  $\alpha=0.05$  ( $n=6-10$ ). IFN, interferon; IDO, indoleamine-2,3-dioxygenase; MFI, median fluorescence intensity; ns, not significant.

an in situ antitumor immune response, is showing considerable promise in early-phase clinical trials.<sup>1-4</sup>

Encouraging results have also been found with intratumoral injection of soluble TLR9 agonists.<sup>50</sup> Despite this, the long-term feasibility of using soluble TLR9 agonists is limited by its sensitivity to nucleases and short half-life.<sup>20</sup> CMP-001 was designed in part to overcome this problem. The Q $\beta$  viral capsid component of CMP-001 is advantageous as it provides protection from nucleases that would be expected to alter the pharmacokinetics and pharmacodynamics of the TLR9 agonist. The VLP construct allows for use of a class A TLR9 agonist that, if given in soluble form, is rapidly degraded by nucleases.<sup>20</sup> The encapsulation of a TLR9 agonist in a Q $\beta$  capsid also impacts on the mechanism

of cellular uptake and likely alters intracellular trafficking patterns of the TLR9 agonist. Optimal cellular uptake of CMP-001 is dependent on opsonization by anti-Q $\beta$  antibody.<sup>3</sup> Uptake of anti-Q $\beta$ -coated CMP-001 has immunological effects independent of the TLR9 agonist it contains.

Despite these differences, there are similarities in mechanisms of action between CMP-001 and soluble TLR9 agonists. Both mediate much of their primary effect by inducing production of type I IFN by pDCs within the TME. This, in turn, induces changes in the TME that ideally lead to abrogation of immune tolerance and development of an active systemic antitumor immune response.

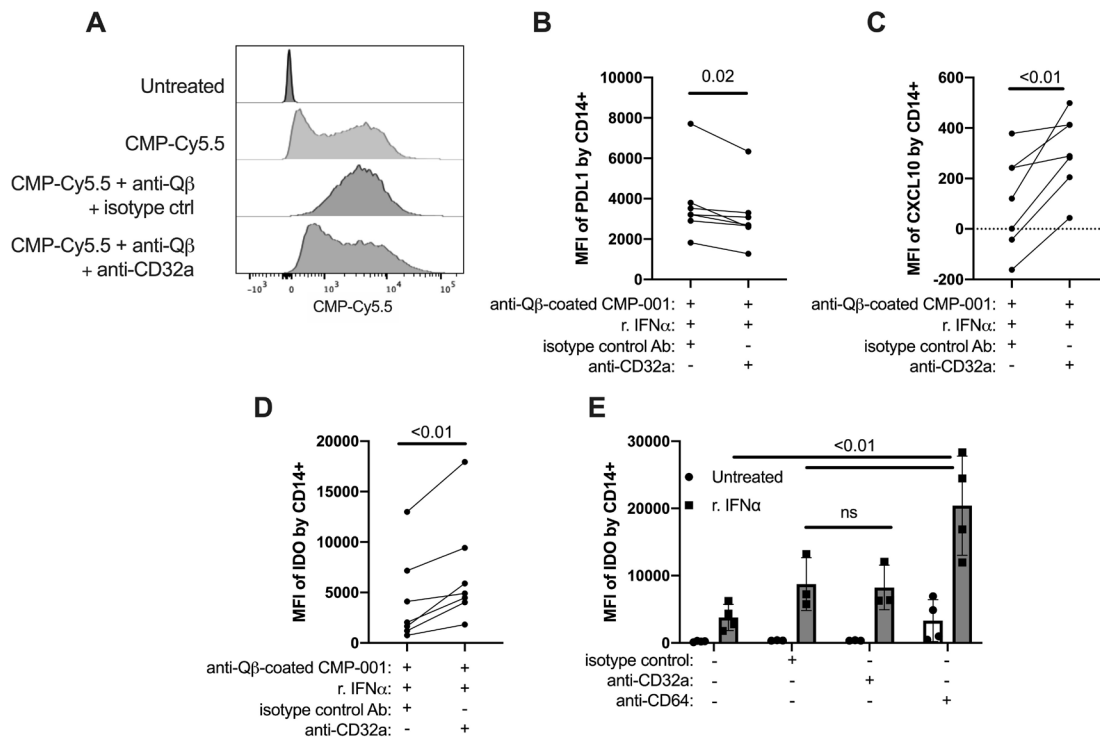


**Figure 6** Impact of CD32a blockade on uptake of anti-Q $\beta$ -coated CMP-001 by monocytes and concomitant response to IFN- $\alpha$ . (A) Monocytes from healthy donors were pretreated anti-CD32a or isotype control for 15 min followed by treatment with 10  $\mu$ g/mL Cy5.5-labeled CMP-001 plus or minus anti-Q $\beta$ . Data are representative of two independent experiments. (B–D) Monocytes from healthy donors were pretreated with anti-CD32a or isotype control for 15 min followed by treatment with recombinant IFN- $\alpha$  and anti-Q $\beta$ -coated CMP-001 for 18–20 hours. Expression of PDL1, CXCL10, and IDO were determined by flow cytometry. (E) Monocytes from healthy donors were treated with 10  $\mu$ g/mL anti-CD32a, anti-CD64, or isotype control (in the absence of particles) for 18–20 hours. Expression of IDO was determined by flow cytometry. Statistical significance was determined using paired t-test (B–D) and two-way analysis of variance (E) with  $\alpha=0.05$  ( $n=3-7$ ). IFN, interferon; IDO, indoleamine-2,3-dioxygenase; MFI, median fluorescence intensity; ns, not significant.

The current studies were designed to better understand the complex response that takes place in the TME following treatment with CMP-001 and to begin the process of distinguishing such changes from those seen with soluble TLR9 agonists. The ultimate goal of this line of research is to enhance our understanding of factors that might help predict response or resistance to CMP-001 therapy and inform development of combination regimens including this novel and promising agent.

We previously reported that pDCs are required for anti-Q $\beta$ -coated CMP-001 to have an immunostimulatory effect and that this effect is mediated in large part by type I IFN production by pDCs.<sup>3</sup> This, in turn, results in an antitumor T-cell response that is responsible for the in vivo efficacy of CMP-001.<sup>3</sup> The studies presented here demonstrate that other myeloid cells, specifically monocytes and related cell types, are also central to the immune response to CMP-001. Monocytes were the most efficient at phagocytosing anti-Q $\beta$ -coated CMP-001. Particles were also taken up by monocytes polarized into classical M1 and M2 macrophages with the understanding that such polarization is an oversimplification of the broad variety of myeloid cell populations seen in the TME. Although such cells take up particles at a level several folds higher than other cell types including pDCs, the direct immunological

impact of CMP-001 on monocytes is relatively modest, in large part because human monocytes do not express TLR9.<sup>7</sup> However, these myeloid cells do respond to type I IFN produced by pDCs in response to CMP-001.<sup>10</sup> ScRNA-seq of unfractionated PBMCs treated with anti-Q $\beta$ -coated CMP-001 demonstrates significant changes in a variety of cells. This includes upregulation of a variety of IFN-response genes in B cells, T cells, NK cells and, most notably, monocytes. Augur analysis, a cell prioritization tool used to identify which cells are most affected by a particular treatment,<sup>32</sup> identified monocytes as being the most responsive to anti-Q $\beta$ -coated CMP-001 treatment.

Together, these data led us to focus on monocytes and related cell types as integral TME components in the efficacy of CMP-001-mediated in situ immunization. Pathway analysis of differentially expressed genes in monocytes after treatment of PBMCs with anti-Q $\beta$ -coated CMP-001 revealed upregulation of IFN-signaling pathways as well as upregulation of pathways involved in communication between innate and adaptive immune cells. These changes were present in multiple cell types but were most prominent in monocytes. These included a variety of molecules well known to be involved in the antitumor immune response such as CXCL10, IDO1 (IDO), and CD274 (PDL1).<sup>3, 33–39</sup>

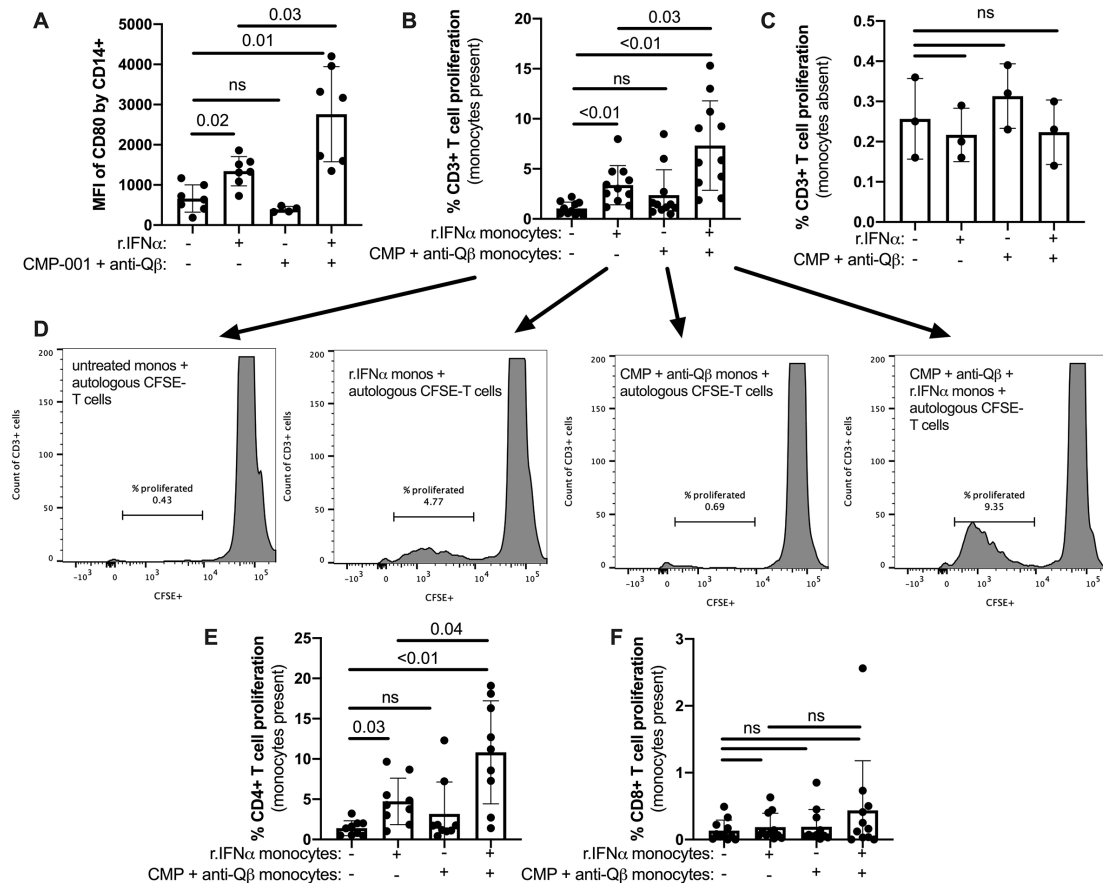


**Figure 7** Monocytes treated with anti-Q $\beta$ -coated CMP-001 and IFN- $\alpha$  upregulate CD80 expression and induce autologous CD4 T-cell proliferation. (A) Monocytes from healthy donors were treated with recombinant IFN- $\alpha$  plus or minus anti-Q $\beta$ -coated CMP-001 for 18–20 hours. CD80 surface expression was determined by flow cytometry. (B) Monocytes from healthy donors were treated with recombinant IFN- $\alpha$  plus or minus anti-Q $\beta$ -coated CMP-001 for 18–20 hours. The next day, autologous CFSE-labeled T cells were added to treated monocytes at a ratio of 1:10 (monocyte:T cell), and percent of CFSE-diluted CD3<sup>+</sup> T cells was determined after 4 days as a measure of T-cell proliferation. (C) Purified CFSE-labeled T cells were treated directly with recombinant IFN- $\alpha$  plus or minus anti-Q $\beta$ -coated CMP-001 in the absence of monocytes, and percent of CFSE-diluted CD3<sup>+</sup> T cells was determined after 4 days as a measure of T-cell proliferation. (D) Representative histograms of CFSE-diluted CD3<sup>+</sup> T cells. (E,F) Phenotypical characterization of proliferated CD3<sup>+</sup> T cells into CD4 and CD8 subsets. Statistical significance was determined using one-way analysis of variance with multiple comparisons test with  $\alpha=0.05$  ( $n=3-11$ ). IFN, interferon; MFI, median fluorescence intensity; ns, not significant.

Though the direct immunological impact of anti-Q $\beta$ -coated CMP-001 on monocytes was modest, uptake of such particles did have a profound impact on their response to IFN- $\alpha$ . These changes were complex and included enhanced expression of IDO and PDL1, and reduced expression of CXCL10. This effect was not TLR9 dependent as it was not seen with naked TLR9. Similar changes were seen after treatment of monocytes with anti-Q $\beta$ -coated VLP lacking a functional TLR9 agonist (mCMP-001) as well as of IgG+ protein L beads, suggesting signaling via Fc gamma receptors alters the monocytic response to IFN- $\alpha$ . Both CD32 and CD64 play a role in how anti-Q $\beta$ -coated CMP-001 impacts the monocyte response to IFN- $\alpha$ . Most notably, anti-Q $\beta$ -coated CMP-001, in the presence of IFN- $\alpha$ , increased monocyte expression of CD80 and enhanced their ability to induce proliferation of autologous CD4<sup>+</sup> T cells.

Overall, these data shed new light on the complex mechanism of action of CMP-001. First, the TLR9 component

of CMP-001 induces production of IFN- $\alpha$  by pDCs in a manner that is dependent on uptake of anti-Q $\beta$ -coated CMP-001.<sup>3</sup> Second, uptake of anti-Q $\beta$ -coated particles alters the monocytic response to IFN- $\alpha$  produced by pDCs and enhances their ability to induce CD4<sup>+</sup> T-cell proliferation. These findings align with previous data showing expansion of CD4<sup>+</sup> T cells in mice secondary to CMP-001 treatment.<sup>3</sup>

In vitro analysis of PBMCs was used as a surrogate for response of the TME to treatment with CMP-001. This approach was selected because PBMCs contain multiple cell types and are highly viable after in vitro culture, thereby allowing for high-quality scRNA-seq. There are obvious limitations to such an approach. No tumor cells were present. Other cell types within the TME including macrophages and fibroblasts were absent, both of which would be expected to influence both the immunosuppressive milieu of the TME and the immune response to

in situ immunization with CMP-001. Despite these limitations, the data presented here provide an important step in understanding the complex immune responses that take place in response to CMP-001. Ongoing in vitro studies are exploring the impact of CMP-001 on the ability of various myeloid subsets to activate T cells. More importantly, in vivo evaluation is needed to help understand these responses more completely. Clinical correlative studies are exploring the impact of CMP-001 on tumor-associated myeloid cells, T cells and other populations obtained from fine needle aspirates and biopsies of patient tumors before and after CMP-001 treatment.

## CONCLUSIONS

We conclude that CMP-001 has complex effects on various immune cell subsets that could impact on its ability to induce an active immune response when delivered intratumorally. CMP-001 is preferentially taken up by monocytes; however, the relatively small amount of CMP-001 that is taken up by pDCs induces production of IFN- $\alpha$  by the pDCs<sup>3</sup> that, in turn, induces changes in multiple cell types, most notably in monocytes. These changes are consistent with the development of a more robust antitumor immune response. Monocytes that have taken up anti-Q $\beta$ -coated CMP-001 have an altered response to IFN- $\alpha$  that is TLR9-independent and mediated via Fc receptor signaling. The observed changes in monocytes provide insight into possible mechanisms by which CMP-001 achieves in vivo efficacy. In addition, such data introduce possible combination treatments with potential to enhance the immune response that results from in situ immunization with CMP-001. For example, these results provide rationale for combining CMP-001 with anti-PD1 therapy and suggest the combination of CMP-001 and IDO inhibition may be worth exploring. An important next step will be confirmation that changes in tumor-associated monocytes/macrophages and related cells from patient samples in response to CMP-001 are consistent with these findings. Graphical abstract of this paper is available in online supplemental file 9.

## Author affiliations

<sup>1</sup>Interdisciplinary Graduate Program in Immunology, The University of Iowa, Iowa City, IA, USA

<sup>2</sup>Medical Scientist Training Program, The University of Iowa Carver College of Medicine, Iowa City, IA, USA

<sup>3</sup>Holden Comprehensive Cancer Center, The University of Iowa, Iowa City, IA, USA

<sup>4</sup>Department of Ophthalmology and Visual Sciences, The University of Iowa Hospitals and Clinics, Iowa City, IA, USA

<sup>5</sup>Laboratory of Systems Pharmacology, Harvard Medical School, Boston, MA, USA

<sup>6</sup>Division of Pharmaceuticals and Translational Therapeutics, The University of Iowa College of Pharmacy, Iowa City, IA, USA

<sup>7</sup>Iowa Institute of Human Genetics, University of Iowa Carver College of Medicine, Iowa City, IA, USA

<sup>8</sup>Department of Internal Medicine, The University of Iowa Hospitals and Clinics, Iowa City, IA, USA

**Acknowledgements** The authors appreciate the support from the University of Iowa Holden Comprehensive Cancer Center and Carver College of Medicine Flow Cytometry, Genomics, and Biostatistics Shared Research Resources. Zhaoming

Wang generously contributed to flow cytometry analyses and Sarah Bell to biostatistical analyses. The authors would like to acknowledge the University of Iowa Institute of Human Genetics (IIHG) Genomics division for 10X scRNA-seq library preparation and sequencing support.

**Contributors** SAS performed the experiments, analyzed the data (excluding the scRNA-seq data), generated the corresponding figures, and wrote the manuscript; APV, MSC and AVI helped analyze the scRNA-seq data. APV additionally performed ingenuity pathway analyses, generated the corresponding scRNA-seq figures, and helped write the manuscript. MSC additionally conducted the Augur analysis. SEB offered robust scientific and technical input for all experiments, helped analyze the data, and helped write the manuscript. GJW provided supervision, offered scientific and technical input for all experiments, helped analyze the data, and helped write the manuscript.

**Funding** Research funding was provided by NIH grants P30 CA86862 and P50 CA97274, including an NCI Diversity Supplement provided to Shakoora Sabree, as well as by funding from Checkmate Pharmaceuticals.

**Competing interests** SEB holds stock options in Checkmate Pharmaceuticals. GJW received research funding from Checkmate Pharmaceuticals. All of the other authors declare no competing interests.

**Patient consent for publication** Not required.

**Provenance and peer review** Not commissioned; externally peer reviewed.

**Data availability statement** Data are available in a public, open access repository. Raw and processed single-cell RNA sequencing data have been deposited in NCBI's Gene Expression Omnibus (GEO) and are available through GEO Series accession numbers GSE162824 and GSE172493. Additionally, processed data are accessible via an interactive web interface (<https://cmp001.shinyapps.io/cmp001/>) using the cellcuratorR R package.

**Supplemental material** This content has been supplied by the author(s). It has not been vetted by BMJ Publishing Group Limited (BMJ) and may not have been peer-reviewed. Any opinions or recommendations discussed are solely those of the author(s) and are not endorsed by BMJ. BMJ disclaims all liability and responsibility arising from any reliance placed on the content. Where the content includes any translated material, BMJ does not warrant the accuracy and reliability of the translations (including but not limited to local regulations, clinical guidelines, terminology, drug names and drug dosages), and is not responsible for any error and/or omissions arising from translation and adaptation or otherwise.

**Open access** This is an open access article distributed in accordance with the Creative Commons Attribution Non Commercial (CC BY-NC 4.0) license, which permits others to distribute, remix, adapt, build upon this work non-commercially, and license their derivative works on different terms, provided the original work is properly cited, appropriate credit is given, any changes made indicated, and the use is non-commercial. See <http://creativecommons.org/licenses/by-nc/4.0/>.

## ORCID iDs

Shakoora A Sabree <http://orcid.org/0000-0001-8392-2112>

George J Weiner <http://orcid.org/0000-0003-3427-0562>

## REFERENCES

- 1 Hammerich L, Bhardwaj N, Kohrt HE, *et al*. In situ vaccination for the treatment of cancer. *Immunotherapy* 2016;8:315–30.
- 2 Cheng Y, Lemke-Miltner CD, Wongpattaraworakul W, *et al*. In situ immunization of a TLR9 agonist virus-like particle enhances anti-PD1 therapy. *J Immunother Cancer* 2020;8:e000940.
- 3 Lemke-Miltner CD, Blackwell SE, Yin C, *et al*. Antibody opsonization of a TLR9 Agonist-Containing virus-like particle enhances in situ immunization. *J Immunol* 2020;204:1386–94.
- 4 Miller AM, Lemke-Miltner CD, Blackwell S, *et al*. Intraperitoneal CMP-001: a novel immunotherapy for treating peritoneal carcinomatosis of gastrointestinal and pancreaticobiliary cancer. *Ann Surg Oncol* 2021;28:1187–97.
- 5 Weiner GJ. CpG oligodeoxynucleotide-based therapy of lymphoid malignancies. *Adv Drug Deliv Rev* 2009;61:263–7.
- 6 Krieg AM. Development of TLR9 agonists for cancer therapy. *J Clin Invest* 2007;117:1184–94.
- 7 Hornung V, Rothenfusser S, Britsch S, *et al*. Quantitative expression of Toll-like receptor 1–10 mRNA in cellular subsets of human peripheral blood mononuclear cells and sensitivity to CpG oligodeoxynucleotides. *J Immunol* 2002;168:4531–7.

- 8 Verthelyi D, Ishii KJ, Gursel M, *et al.* Human peripheral blood cells differentially recognize and respond to two distinct CpG motifs. *J Immunol* 2001;166:2372–7.
- 9 Gürsel M, Verthelyi D, Gürsel I, *et al.* Differential and competitive activation of human immune cells by distinct classes of CpG oligodeoxynucleotide. *J Leukoc Biol* 2002;71:813–20.
- 10 Blackwell SE, Krieg AM. CpG-A-induced monocyte IFN-gamma-inducible protein-10 production is regulated by plasmacytoid dendritic cell-derived IFN-alpha. *J Immunol* 2003;170:4061–8.
- 11 Yang X, Zhang X, Fu ML, *et al.* Targeting the tumor microenvironment with interferon- $\beta$  bridges innate and adaptive immune responses. *Cancer Cell* 2014;25:37–48.
- 12 Mohty M, Vialle-Castellano A, Nunes JA, *et al.* Ifn-Alpha skews monocyte differentiation into Toll-like receptor 7-expressing dendritic cells with potent functional activities. *J Immunol* 2003;171:3385–93.
- 13 Korthals M, Safaian N, Kronenwett R, *et al.* Monocyte derived dendritic cells generated by IFN-alpha acquire mature dendritic and natural killer cell properties as shown by gene expression analysis. *J Transl Med* 2007;5:46.
- 14 Ruan M, Thorn K, Liu S, *et al.* The secretion of IL-6 by CpG-ODN-treated cancer cells promotes T-cell immune responses partly through the TLR-9/AP-1 pathway in oral squamous cell carcinoma. *Int J Oncol* 2014;44:2103–10.
- 15 van den Hout MFCM, Sluijter BJR, Santegoets SJAM, *et al.* Local delivery of CpG-B and GM-CSF induces concerted activation of effector and regulatory T cells in the human melanoma sentinel lymph node. *Cancer Immunol Immunother* 2016;65:405–15.
- 16 Marshall JD, Fearon K, Abbate C, *et al.* Identification of a novel CpG DNA class and motif that optimally stimulate B cell and plasmacytoid dendritic cell functions. *J Leukoc Biol* 2003;73:781–92.
- 17 Ribas A, Medina T, Kummar S, *et al.* SD-101 in combination with pembrolizumab in advanced melanoma: results of a phase Ib, multicenter study. *Cancer Discov* 2018;8:1250–7.
- 18 Milhem M, Zakharia Y, Davar D. 304 Intratumoral injection of CMP-001, a toll-like receptor 9 (TLR9) agonist, in combination with pembrolizumab reversed programmed death receptor 1 (PD-1) blockade resistance in advanced melanoma. *JITC* 2020;8:A331.
- 19 Link BK, Ballas ZK, Weisdorf D, *et al.* Oligodeoxynucleotide CpG 7909 delivered as intravenous infusion demonstrates immunologic modulation in patients with previously treated non-Hodgkin lymphoma. *J Immunother* 2006;29:558–68.
- 20 Meng W, Yamazaki T, Nishida Y, *et al.* Nuclease-Resistant immunostimulatory phosphodiester CpG oligodeoxynucleotides as human Toll-like receptor 9 agonists. *BMC Biotechnol* 2011;11:88.
- 21 Mohsen M, Gomes A, Vogel M, *et al.* Interaction of viral Capsid-Derived virus-like particles (VLPs) with the innate immune system. *Vaccines* 2018;6:37.
- 22 Gomes AC, Mohsen M, Bachmann MF. Harnessing nanoparticles for immunomodulation and vaccines. *Vaccines* 2017;5. doi:10.3390/vaccines5010006. [Epub ahead of print: 14 Feb 2017].
- 23 Davar D, Karunamurthy A, Hartman D. 303 Phase II trial of neoadjuvant nivolumab (Nivo) and intra-tumoral (IT) CMP-001 in high-risk resectable melanoma (Neo-C-Nivo): final results. *JITC* 2020;8:A330-A.
- 24 Morris A, Walters E, Akache B. 604 Intravenous CMP-001, a CpG-A Toll-like receptor 9 (TLR9) agonist delivered via a virus-like particle, causes tumor regression in syngeneic Hepa1–6 mouse models of hepatocellular carcinoma. *JITC* 2020;8:A639-A.
- 25 Böyum A. Isolation of mononuclear cells and granulocytes from human blood. Isolation of mononuclear cells by one centrifugation, and of granulocytes by combining centrifugation and sedimentation at 1 G. *Scand J Clin Lab Invest Suppl* 1968;97:77–89.
- 26 Zarif JC, Hernandez JR, Verdone JE, *et al.* A phased strategy to differentiate human CD14+monocytes into classically and alternatively activated macrophages and dendritic cells. *Biotechniques* 2016;61:33–41.
- 27 Zheng GXY, Terry JM, Belgrader P, *et al.* Massively parallel digital transcriptional profiling of single cells. *Nat Commun* 2017;8:14049.
- 28 Butler A, Hoffman P, Smibert P, *et al.* Integrating single-cell transcriptomic data across different conditions, technologies, and species. *Nat Biotechnol* 2018;36:411–20.
- 29 Stuart T, Butler A, Hoffman P, *et al.* Comprehensive integration of single-cell data. *Cell* 2019;177:1888–902.
- 30 Zhu L, Yang P, Zhao Y, *et al.* Single-Cell sequencing of peripheral mononuclear cells reveals distinct immune response landscapes of COVID-19 and influenza patients. *Immunity* 2020;53:685–96.
- 31 Hashimoto K, Kouno T, Ikawa T, *et al.* Single-Cell transcriptomics reveals expansion of cytotoxic CD4 T cells in supercentenarians. *Proc Natl Acad Sci U S A* 2019;116:201907883.
- 32 Skinnider MA, Squair JW, Kathe C, *et al.* Cell type prioritization in single-cell data. *Nat Biotechnol* 2021;39:30–4.
- 33 House IG, Savas P, Lai J, *et al.* Macrophage-Derived CXCL9 and CXCL10 are required for antitumor immune responses following immune checkpoint blockade. *Clin Cancer Res* 2020;26:487–504.
- 34 Huang H, Liu Y, Xiang J. Synergistic effect of adoptive T-cell therapy and intratumoral interferon gamma-inducible protein-10 transgene expression in treatment of established tumors. *Cell Immunol* 2002;217:12–22.
- 35 Padovan E, Spagnoli GC, Ferrantini M, *et al.* IFN-alpha2a induces IP-10/CXCL10 and MIG/CXCL9 production in monocyte-derived dendritic cells and enhances their capacity to attract and stimulate CD8+ effector T cells. *J Leukoc Biol* 2002;71:669–76.
- 36 Yang H, Yamazaki T, Pietroccola F, *et al.* Stat3 inhibition enhances the therapeutic efficacy of immunogenic chemotherapy by stimulating type 1 interferon production by cancer cells. *Cancer Res* 2015;75:3812–22.
- 37 Munn DH. Indoleamine 2,3-dioxygenase, tumor-induced tolerance and counter-regulation. *Curr Opin Immunol* 2006;18:220–5.
- 38 Nakamura N, Hara T, Shimizu M, *et al.* Effects of indoleamine 2,3-dioxygenase inhibitor in non-Hodgkin lymphoma model mice. *Int J Hematol* 2015;102:327–34.
- 39 Chen B, Alvarado DM, Ilicovici M, *et al.* Interferon-Induced IDO1 mediates radiation resistance and is a therapeutic target in colorectal cancer. *Cancer Immunol Res* 2020;8:451–64.
- 40 Voigt AP, Whitmore SS, Lessing ND, *et al.* Spectacle: an interactive resource for ocular single-cell RNA sequencing data analysis. *Exp Eye Res* 2020;200:108204.
- 41 Fallarino F, Puccetti P. Toll-Like receptor 9-mediated induction of the immunosuppressive pathway of tryptophan catabolism. *Eur J Immunol* 2006;36:8–11.
- 42 Jacquelot N, Yamazaki T, Roberti MP, *et al.* Sustained type I interferon signaling as a mechanism of resistance to PD-1 blockade. *Cell Res* 2019;29:846–61.
- 43 Vollmer J, Jurk M, Samulowitz U, *et al.* CpG oligodeoxynucleotides stimulate IFN-gamma-inducible protein-10 production in human B cells. *J Endotoxin Res* 2004;10:431–8.
- 44 Ohmori Y, Hamilton TA. The interferon-stimulated response element and a kappa B site mediate synergistic induction of murine IP-10 gene transcription by IFN-gamma and TNF-alpha. *J Immunol* 1995;154:5235–44.
- 45 Burke SJ, Goff MR, Lu D, *et al.* Synergistic expression of the CXCL10 gene in response to IL-1 $\beta$  and IFN- $\gamma$  involves NF- $\kappa$ B, phosphorylation of STAT1 at Tyr701, and acetylation of histones H3 and H4. *J Immunol* 2013;191:323–36.
- 46 Qi X-F, Kim D-H, Yoon Y-S, *et al.* Essential involvement of cross-talk between IFN-gamma and TNF-alpha in CXCL10 production in human THP-1 monocytes. *J Cell Physiol* 2009;220:690–7.
- 47 Finotti G, Tamassia N, Calzetti F, *et al.* Endogenously produced TNF- $\alpha$  contributes to the expression of CXCL10/IP-10 in IFN- $\lambda$ 3-activated plasmacytoid dendritic cells. *J Leukoc Biol* 2016;99:107–19.
- 48 Piehler J, Thomas C, Garcia KC, *et al.* Structural and dynamic determinants of type I interferon receptor assembly and their functional interpretation. *Immunol Rev* 2012;250:317–34.
- 49 Båve U, Magnusson M, Eloranta M-L, Perers A, *et al.* Fc gamma RIIA is expressed on natural IFN-alpha-producing cells (plasmacytoid dendritic cells) and is required for the IFN-alpha production induced by apoptotic cells combined with lupus IgG. *J Immunol* 2003;171:3296–302.
- 50 Brody JD, Ai WZ, Czerwinski DK, *et al.* In situ vaccination with a TLR9 agonist induces systemic lymphoma regression: a phase I/II study. *JCO* 2010;28:4324–32.